

Stabilization of the Actomyosin Ring Enables Spermatocyte Cytokinesis in *Drosophila*

Philip Goldbach,^{*†} Raymond Wong,^{*‡} Nolan Beise,^{§||} Ritu Sarpal,[¶]
William S. Trimble,^{§||} and Julie A. Brill^{*†‡}

^{*}Program in Developmental and Stem Cell Biology, The Hospital for Sick Children, Toronto, ON, M5G 1L7, Canada; [†]Department of Molecular Genetics, and [‡]Institute of Medical Science, and ^{||}Department of Biochemistry, University of Toronto, Toronto, ON, M5S 1A8, Canada; [§]Program in Cell Biology, The Hospital for Sick Children, Toronto, ON, M5G 1X8, Canada; and [¶]Department of Cell and Systems Biology, University of Toronto, Toronto, ON M5S 3G5, Canada

Submitted August 20, 2009; Revised January 25, 2010; Accepted March 5, 2010
Monitoring Editor: Fred Chang

The scaffolding protein anillin is required for completion of cytokinesis. Anillin binds filamentous (F) actin, nonmuscle myosin II, and septins and in cell culture models has been shown to restrict actomyosin contractility to the cleavage furrow. Whether anillin also serves this function during the incomplete cytokinesis that occurs in developing germ cells has remained unclear. Here, we show that anillin is required for cytokinesis in dividing *Drosophila melanogaster* spermatocytes and that anillin, septins, and myosin II stably associate with the cleavage furrow in wild-type cells. Anillin is necessary for recruitment of septins to the cleavage furrow and for maintenance of F-actin and myosin II at the equator in late stages of cytokinesis. Remarkably, expression of DE-cadherin suppresses the cytokinesis defect of anillin-depleted spermatocytes. DE-cadherin recruits β -catenin (armadillo) and α -catenin to the cleavage furrow and stabilizes F-actin at the equator. Similarly, E-cadherin expression suppresses the cytokinesis defect caused by anillin knockdown in mouse L-fibroblast cells. Our results show that the anillin-septin and cadherin-catenin complexes can serve as alternative cassettes to promote tight physical coupling of F-actin and myosin II to the cleavage furrow and successful completion of cytokinesis.

INTRODUCTION

Cytokinesis has long been recognized to involve formation and constriction of a contractile ring composed of filamentous (F) actin and nonmuscle myosin II (Satterwhite and Pollard, 1992; Rappaport, 1996). Bipolar filaments of myosin II are thought to draw F-actin together in a purse-string like manner to constrict the contractile ring. Studies in yeast and mammalian cells suggest that actin and myosin turn over during constriction, leading to an idea that F-actin and myosin are constantly recruited and disassembled at the cleavage furrow during cytokinesis (Pelham and Chang, 2002; Murthy and Wadsworth, 2005). However, recent work in the early *Caenorhabditis elegans* embryo suggests that actin and myosin do not turn over, but rather disassemble over time (Carvalho *et al.*, 2009). In either case, a tight link must be established between the actomyosin ring and the plasma membrane at the equator, and this attachment must be maintained during late stages of cytokinesis.

Among the proteins thought to link the actomyosin ring to the equator are septin filaments, which form a gauze-like structure that is tightly associated with cellular membranes (Rodal *et al.*, 2005). The mammalian septin SEPT2 binds myosin II, and this association is required for myosin activation during cell division (Joo *et al.*, 2007). Septins do not interact directly with F-actin, but rather associate indirectly

through anillin, a scaffolding protein that links these cytoskeletal components with microtubules and Rho at the equator (reviewed in D'Avino, 2009). Thus, anillin can be thought of as promoting formation of a stable plasma membrane-associated complex that anchors F-actin to the cell cortex during cleavage. Other analogous complexes that link F-actin to the plasma membrane include adherens junctions, which are composed of E-cadherin and α - and β -catenin (Hartsock and Nelson, 2008; Miyoshi and Takai, 2008).

Anillin was originally identified in *Drosophila melanogaster* embryo extracts as an actin-binding and -bundling protein that localizes to the cleavage furrow during cytokinesis (Miller *et al.*, 1989; Field and Alberts, 1995). Subsequent studies showed that anillin binds myosin II and septins and promotes septin recruitment to the cleavage furrow in *Xenopus laevis* and mammalian cells (Oegema *et al.*, 2000; Kinoshita *et al.*, 2002; Straight *et al.*, 2005). Anillin homologues in the fission yeast *Schizosaccharomyces pombe* are involved in establishment of the plane of cleavage and in organizing and stabilizing septins at the medial ring (Chang *et al.*, 1996; Sohrmann *et al.*, 1996; Berlin *et al.*, 2003; Tasto *et al.*, 2003). In animal cells, depletion of anillin by RNA interference (RNAi) results in cytokinesis failure in late telophase (Somma *et al.*, 2002; Echard *et al.*, 2004; Straight *et al.*, 2005; Zhao and Fang, 2005; D'Avino *et al.*, 2008; Piekny and Glotzer, 2008). Loss of anillin is associated with delocalized actomyosin contractility, with myosin regulatory light chain (Spaghetti squash or Sqh in *Drosophila*) moving around the periphery of the cell rather than remaining concentrated at the equator (Straight *et al.*, 2005; Hickson and O'Farrell, 2008; Piekny and Glotzer, 2008). Anillin is postulated to constrain activated myosin at the cleavage furrow by binding myosin

This article was published online ahead of print in *MBoC in Press* (<http://www.molbiolcell.org/cgi/doi/10.1091/mbc.E09-08-0714>) on March 17, 2010.

Address correspondence to: Julie A. Brill (julie.brill@sickkids.ca).

II, F-actin, and the septins. Moreover, anillin binds the small GTPase Rho and RacGAP and may thus facilitate Rho-mediated actin assembly via formins and myosin contractility via Rho kinase (D'Avino *et al.*, 2008; Gregory *et al.*, 2008; Piekny and Glotzer, 2008). Notably, because many of the published experiments describing anillin function have been carried out in tissue culture models, relatively little is known about anillin function in a multicellular organism *in vivo*.

The majority of anillin studies in multicellular model organisms have been conducted in *C. elegans* and *Drosophila*. In *C. elegans*, which has three anillin-related proteins, ANI-1 is required for early actomyosin-based contractile events in the embryo, for recruitment of septins to contractile rings, and for a symmetry-breaking event associated with initiation of cleavage at the first embryonic division (Maddox *et al.*, 2005, 2007). In *Drosophila* embryos, binding of anillin to septins is required to maintain integrity of the invaginating cellular membranes during cellularization—a modified form of cytokinesis—and for conventional cytokinesis in later stages of embryonic development (Field *et al.*, 2005). Indeed, anillin has recently been shown to be required for cytokinesis and asymmetric cell division in the *Drosophila* peripheral nervous system (O'Farrell and Kylsten, 2008). However, with the exception of septin recruitment, the mechanism by which anillin promotes conventional cytokinesis in a multicellular organism remains unknown.

To examine anillin function *in vivo*, we focused on meiotic cytokinesis in *Drosophila* spermatocytes and on later stages during differentiation of mature sperm. Spermatocytes provide an excellent system for studying animal cell cytokinesis because they are large, their mechanism of cytokinesis is conserved with other animal cells, and they are amenable to manipulation using powerful molecular genetic techniques (Fuller, 1993; Giansanti *et al.*, 2001). Germ cell cytokinesis is incomplete, and developing male germ cells remain connected by stable intercellular bridges called ring canals. Syncytial cysts of 16 primary spermatocytes form by mitotic divisions of a gonial cell precursor. All 16 spermatocytes undergo meiotic cytokinesis, forming cysts of 64 interconnected spermatids that share a common cytoplasm. During differentiation, spermatids elongate and form needle-shaped nuclei. Mature sperm arise by individualization of mature spermatids via an actin-based process. Sixty-four actin-based investment cones form over the nuclei and, in a myosin VI-dependent manner, traverse the nearly 2-mm-long tails, investing each sperm with its own plasma membrane (Fabrizio *et al.*, 1998; Hicks *et al.*, 1999). In earlier studies, anillin was shown to be one of the first markers to appear at the equator of dividing spermatocytes (Hime *et al.*, 1996; Giansanti *et al.*, 1999). After cytokinesis, anillin and the septins persist in stable intercellular bridges that localize to the growing end of elongating cysts of haploid spermatids (Hime *et al.*, 1996). Importantly, these localization studies did not address the function of anillin in male germ cell development.

Here, we examine anillin localization and function in developing male germ cells. We find that anillin is required for male germ cell cytokinesis. Anillin functions to localize septins to the cleavage furrow and to maintain Rho, F-actin, and myosin in the contractile ring. We show that expression of DE-cadherin (DE-cad) suppresses the cytokinesis defect caused by loss of anillin. DE-cad recruits other cadherin-catenin complex proteins to the cleavage furrow and stabilizes contractile ring F-actin in anillin-depleted cells. Thus, DE-cad and anillin and their respective binding partners form alternative cassettes that anchor actin at the cell equator, enabling successful cytokinesis.

MATERIALS AND METHODS

Molecular Biology

Molecular cloning was performed using standard techniques (Sambrook *et al.*, 1989). Restriction enzymes and T4 DNA ligase were from New England Biolabs (Ipswich, MA). PCR was performed using Phusion DNA Polymerase (Finnzymes, New England Biolabs) on an MJ Research PTC-200 PCR machine (Waltham, MA).

Plasmids for generating transgenic flies were made in the P element transformation vector *tv3*, which contains the spermatocyte-specific β_2 -tubulin (β_2t) promoter and SV40 3' sequences (Wong *et al.*, 2005), or in pCaSpeR-tub::mCherry, a modified version of pCaSpeR4 (Pirrota, 1988) containing the α_1 -tubulin promoter (generously provided by H. Krämer [University of Texas Southwestern Medical Center, Dallas, TX]; Marois *et al.*, 2006) fused to mCherry (generously provided by R. Tsien [University of California, San Diego, La Jolla, CA]; Shaner *et al.*, 2004; J. Burgess and J. A. Brill, unpublished data). A snapback RNAi construct (Kalidas and Smith, 2002) directed against *anillin*, *tv3::anillin-RNAi*, was generated as an antiparallel genomic DNA-cDNA fusion, using the genomic BAC clone BACR04H12 (BACPAC Resources, Children's Hospital Oakland Research Institute, Oakland, CA) and the *anillin* cDNA LD23793 (Berkeley *Drosophila* Genome Project, DGC Release 1) as templates for PCR amplification of 690 base pairs (genomic) or 530 base pairs (cDNA) encoding part of exon7 through exon 9.

tv3::mRFP-anillin and *tv3::GFP-anillin* were made by fusing monomeric red fluorescent protein 1 (mRFP1; a gift from R. Tsien; Campbell *et al.*, 2002) or monomeric enhanced green fluorescent protein (mEGFP; courtesy of E. Snapp [National Institutes of Health, Bethesda, MD]; Zacharias *et al.*, 2002) to the amino terminus of the full-length *anillin* cDNA LD23793. The calponin homology domain of utrophin (Utr-CH) was amplified from GFP-Utr-CH (kindly provided by B. Burkel and W. Bement [University of Wisconsin, Madison, WI]; Burkel *et al.*, 2007) and used to generate pCaSpeR-tub::mCherry-Utr-CH. All constructs were confirmed by DNA sequencing (The Centre for Applied Genomics, The Hospital for Sick Children). Details of molecular cloning (primers, restriction sites, and sequences) will be provided upon request.

Generation of Anti-Anillin Antibody

Polyclonal antisera were raised against the N-terminal portion of anillin as previously described (Field and Alberts, 1995), with the exception that the corresponding sequence of cDNA LD23793 encodes an additional 36 amino acids. DNA sequences encoding the N-terminal 409 amino acids were amplified by PCR and cloned into pGEX-4T-1 (GE Healthcare, Little Chalfont, Buckinghamshire, United Kingdom), expressed in BL21[DE3] bacterial cells as a glutathione S-transferase (GST) fusion (GST-anil¹⁻⁴⁰⁹), purified using Poly-Prep Chromatography Columns (Bio-Rad, Hercules, CA) packed with glutathione Sepharose beads (GE Healthcare; glutathione Sepharose 4B), and eluted with glutathione (Sigma, St. Louis, MO). Two rabbits were injected at The Hospital for Sick Children Lab Animal Services using standard procedures. IgGs were purified from rabbit serum using protein A beads (Bio-Rad; Affi-Gel protein A gel), depleted for anti-GST reactivity, affinity-purified against GST-anil¹⁻⁴⁰⁹ using Affigel-10 columns (Bio-Rad; Affi-Gel 10), and tested for specificity by immunoblotting and immunofluorescence. Antibody 4091 was used at 1:1000 and 1:100 for immunoblotting and immunofluorescence, respectively.

Drosophila Genetics

Flies were raised on standard cornmeal molasses agar at 25°C (Ashburner, 1990). Transgenes were introduced by injection of *w¹¹¹⁸* embryos as described (Wong *et al.*, 2005). Stocks used in the generation of male germ cell clones were obtained from the Bloomington *Drosophila* Stock Center (Bloomington, IN): *P[neoFRT]42D*; *ry⁶⁰⁵, w¹¹¹⁸*; *P[neoFRT]42D P[Ubi-GFP(S65T)^{NLS}]2R/CyO*, *y¹ w¹¹¹⁸ P[70FLP]3F/Dp(1;Y)y⁺; noc^{Sc0}/SM6a*, and *P[PZ]anil⁰³⁴²⁷, cn¹/CyO*; *ry⁵⁰⁶*, a P[PZ] insertion 53 bp upstream of the start codon (*anil^{PZ}*; Doberstein *et al.*, 1997; Field *et al.*, 2005). To make clones, flies were heat-shocked at 37°C for 1 h daily until pupariation. UAS::*anillin-RNAi* flies were from the Vienna *Drosophila* RNAi Collection (VDRC 33465). Fly stocks were as follows: *Bam-GAL4* (gift of D. McKearin [University of Texas Southwestern Medical Center, Dallas, TX]; Chen and McKearin, 2003); *Sep2-GFP* (gift of K. Hales, Davidson College; Silverman-Gavrila *et al.*, 2008); *ubiquitin::DE-cad-GFP* (provided by H. Oda via U. Tepass, University of Toronto; Oda and Tsukita, 2001); *Sqh-GFP* (gift of R. Kares [Institut Jacques Monod, CNRS, University of Paris, Paris, France]; Royou *et al.*, 2002); $\beta_2t::CLC-GFP$ (gift of H. Chang, Purdue University). Flies expressing a secreted GFP (Pfeiffer *et al.*, 2000) under control of the β_2t promoter (Wilson *et al.*, 2006) have been described elsewhere (Polevoy *et al.*, 2009). *GFP^{NLS}* flies used as controls in the DE-cad-GFP rescue experiment were the same as those used in generating germ cell clones (see above). *fud³/TM6B* and *Df(3L)7C/TM6B* were previously described (Brill *et al.*, 2000). *w¹¹¹⁸* flies were used as wild-type controls.

Fluorescence Microscopy, Imaging, and Analysis

Immunofluorescence was performed essentially as described (Hime *et al.*, 1996), except that testis isolation buffer (TIB; Casal *et al.*, 1990) was used instead of TB-1. Unless specified, samples were fixed in PBS (pH 7.2) with 4%

paraformaldehyde followed by permeabilization in PBS with 0.3% Triton X-100 and 0.3% sodium deoxycholate. For anti-DE-cad, anti-armadillo, and anti- α -catenin, salt-free phosphate buffer (PB), pH 7.4, was used instead of PBS, and permeabilization was performed in PB plus 0.3% Triton X-100 (Nievadomska *et al.*, 1999). Antibodies used were as follows: 1:100 rabbit anti-anillin (see above), 1:20 mouse anti-myosin VI (3C7, a gift of K. Miller [Washington University, St. Louis, MO]; Kellerman and Miller, 1992), 1:150 mouse anti-peanut (4C9H4; Developmental Studies Hybridoma Bank [DSHB], Iowa City, IA; Neufeld and Rubin, 1994), 1:100 mouse anti-Rho (p1D9, DSHB; Magie *et al.*, 2002), 1:50 rat anti-DE-cad (gift of U. Tepass [University of Toronto, Toronto, Canada]; Oda *et al.*, 1994), 1:50 mouse anti-armadillo (N2 7A1, DSHB; Riggleman *et al.*, 1990), and 1:5000 guinea pig anti- α -catenin (unpublished data). Rhodamine phalloidin (20 U/ml) and DAPI (1:1000 from 5 mg/ml stock) were used as recommended by the manufacturer (Molecular Probes, Eugene, OR).

To image live squashed preparations of *Drosophila* male germ cells expressing fluorescent fusion proteins (Sqh-GFP, mCherry-Utr-CH), testes were dissected in TIB, transferred to a microscope slide, and cut with tungsten needles in TIB containing 8.3 μ g/ml Hoechst 33342 (Sigma) to stain DNA. Samples were squashed with a coverslip before viewing. Live images of dividing spermatocytes were acquired at 20-s intervals from cells prepared using the clot technique (Wong *et al.*, 2005). Playback speed in the Supplemental Videos is 5 frames per second. Time zero in the figures was arbitrarily set at an equivalent stage of cytokinesis across all genotypes.

Phase-contrast and fluorescence images were acquired with a Zeiss Axio-cam CCD camera on an upright Zeiss AxioPlan 2 microscope using Axiovision software (Zeiss, Oberkochen, Germany). Images of separate fluorochromes from multiply stained tissues were collected individually and combined using Adobe Photoshop (San Jose, CA). When necessary, images were adjusted only for brightness and contrast. Unless otherwise stated, in cases in which direct comparison of images was required, images were acquired using identical exposure times and adjusted in an identical manner.

Fluorescence Recovery after Photobleaching Image Acquisition and Data Analysis

Fluorescence recovery after photobleaching (FRAP) was performed on live cells prepared as described (Wong *et al.*, 2005), using a Zeiss Axiovert 200 equipped with a Hamamatsu C9100-13 EM-CCD camera (Bridgewater, NJ), Yokogawa spinning disk confocal scan head (Tokyo, Japan), diode-pumped solid-state laser lines (Spectral Applied Research: 405, 491, 561, and 638 nm; Richmond Hill, ON, Canada) and a Ludl motorized XY stage (Hawthorne, NY). Images were acquired with a 63 \times /1.3 Zeiss Plan Apo water-immersion objective, with an additional 1.5 \times magnification lens in front of the camera. Photobleaching was performed using the Photonic Instruments (St. Charles, IL) Mosaic FRAP illuminator (488 nm). Acquisition and analysis were performed using Improvision Volocity 5 (PerkinElmer, Waltham, MA).

Bleaching was performed on one visible edge of the cleavage furrow, where the opposite edge was used as an internal, unbleached control. Volocity FRAP analysis software was used to measure the $t_{1/2}$ values for the PLC δ -PH-GFP marker. GFP images were corrected for photobleaching in Volocity. Circular regions of interest of 2- μ m diameter were centered on the visible edges of cleavage furrows for bleached and unbleached sides at each time point. Mean fluorescence intensity values were measured in Volocity and transferred to Microsoft Excel (Redmond, WA). Fluorescence intensity values were normalized using the equation: $(y^x - y^{\min}) / (y^{\max} - y^{\min})$, where y is mean fluorescence intensity and y^x is the value of y at a given time point (x). Graphs were generated in Microsoft Excel. For GFP-anil, Sep2-GFP, and Sqh-GFP, percentage recovery was calculated by taking the mean fluorescence intensity value of six individual values centered on 5 min after bleaching, normalizing against unbleached values, and dividing by the prebleached value.

Immunoblotting

For testis blots, 25 pairs of testes per genotype were dissected in TIB and then transferred directly to SDS-PAGE sample buffer and boiled for 5 min. Proteins were separated on 10% SDS polyacrylamide gels and transferred to Amersham Hybond-ECL nitrocellulose membranes (GE Healthcare) using a Hoefer miniVE system (Hoefer, San Francisco, CA). Blocking and antibody incubations were in Tris-buffered saline with 0.05% Tween-20 (TBST) containing 4% nonfat dry milk (Bio-Rad; Blotting Grade Blocker 170-6404). Washes were in TBST. Primary antibodies were used at the following dilutions: anti-anillin (1:1000), anti-armadillo (1:500), anti- α -catenin (1:5000), anti- β -tubulin N-357 (Amersham, GE Healthcare; 1:4000). HRP-conjugated secondary antibodies (Jackson ImmunoResearch Laboratories, West Grove, PA) were used at 1:10,000. Signals were detected using Amersham ECL Plus Western Blotting Detection Reagents. For L-cell blots, 20 μ g of lysate/condition was run on a 10% SDS polyacrylamide gel at 100 V for 1.5 h, transferred at 250 mA for 2 h onto PVDF membrane, and then blocked in 5% skim milk powder in TBST overnight (O/N). Anillin was visualized with rabbit anti-anillin antibody (1:20,000), generated as described (Oegema *et al.*, 2000), or mouse monoclonal anti-GAPDH (1:40,000; Millipore, Billerica, MA) in TBST. Blots were washed O/N in TBST, incubated with HRP-conjugated anti-rabbit or anti-mouse (1:5000; Jackson ImmunoResearch) for 1 h, and then washed three times with TBST. Blots were imaged with standard ECL reagents (Amersham).

Mammalian Cell Culture and Transfection

Mouse LP (vector only) and LE (E-cadherin expressing) cells were a gift of J. Nelson (Stanford University School of Medicine, Stanford, CA; Angres *et al.*, 1996). LP and LE cells (<3 wk old) were plated in DMEM containing 5% fetal bovine serum and 300 μ g/ml G418 at 60–80% confluency (Wisent, St. Bruno, QC, Canada). Cells were incubated overnight and then cotransfected via Fugene HD (Roche, Basel, Switzerland) with 1 μ g pEGFP1 (Clontech, Mountain View, CA) and either 3 μ g of pSUPER-anillin (anillin knockdown [Anil KD]) or 3 μ g of a nonspecific short hairpin RNA (shRNA) sequence (Ctrl KD) per two wells of a six-well plate. Two anillin shRNA sequences were cloned into pSUPER (Oligoengine, Seattle, WA) to make knockdown (KD) constructs: 5'-CGCAACACTCTGGAATTGATTTC-3' and 5'-GCAGGTTGATTCTATGCTTTC-3'. LP and LE cells were incubated overnight, and then each well was replated into three wells in standard media with 1 μ g/ml dexamethasone (Sigma) for both Ctrl and Anillin knockdowns to induce E-cadherin overexpression selectively in LE cells, as previously described (Angres *et al.*, 1996). After 2 d of incubation, cells were fixed and stained with Hoechst 33342 (Sigma; 1:5000) in PBS. Cells cotransfected with pEGFP1 and pSUPER-shRNA knockdown construct (green cells) were scored for polyploidy: transfected cells with >1 nucleus in interphase were counted as multinucleate. Cells with one nucleus were counted as normal. One hundred cells were counted per condition in triplicate with three replicates (3n) for the Ctrl knockdown and 6n for Anil KD.

RESULTS

Anillin Is Found in a Variety of Actin-associated Structures during Spermatogenesis

Anillin was previously reported to localize to contractile rings and ring canals during spermatogenesis (Hime *et al.*, 1996; Giansanti *et al.*, 1999). To further characterize anillin localization, we generated a new polyclonal antibody using an epitope similar to that previously described by Field *et al.* (1995; see *Materials and Methods*). Immunostaining of developing male germ cells with anti-anillin antibody revealed anillin localization to mitotic ring canals (Figure 1A), mitotic and meiotic contractile rings (not shown and Figure 1B) and ring canals at the growing ends of elongating spermatid cysts (Figure 1, C and D). In addition, anillin localized to the dense body, an actin- and tubulin-rich structure that associates with haploid nuclei during nuclear shaping (Figure 1, D and E). During investment cone formation, anillin was found in puncta near the investment cones (Figure 1F). In cysts in which the investment cones started to move away from the nuclei, anillin puncta appeared to coalesce (Figure 1G), becoming highly concentrated at the leading edge of mature cones as they traversed the length of individualizing cysts (Figure 1H). Anti-anillin antibody staining was specific, as the signal was largely absent from male germ cells depleted for anillin (see below). Thus, anillin is highly concentrated in several actin-rich structures in developing male germ cells.

Anillin Is Required for Spermatocyte Cytokinesis

To test whether anillin is required for cytokinesis, ring canal maintenance or investment cone formation, we generated clones of male germ cells homozygous for a lethal P element insertion in *anillin* (*anil*^{PZ}). Unlike wild-type spermatids (Figure 2A), *anil*^{PZ} mutant spermatids (Figure 2B) were multinucleate, indicating a defect in male meiotic cytokinesis (Romrell *et al.*, 1972). To confirm that this was due to the *anil*^{PZ} mutation, we expressed a translational mRFP fusion to anillin, which fully rescued the cytokinesis defect of *anil*^{PZ} mutant clones (Figure 2C).

To further explore the requirement for anillin in cytokinesis, we used RNAi induced by expression of double-stranded RNA (dsRNA) directed against sequences from the *anillin* gene (see *Materials and Methods*). Two different dsRNAs were used: one under control of the primary spermatocyte-specific β_2 -tubulin promoter (Hoyle and Raff, 1990; Wong *et al.*, 2005) and the other a UAS-dsRNA construct obtained from the Vienna *Drosophila* RNAi Center and

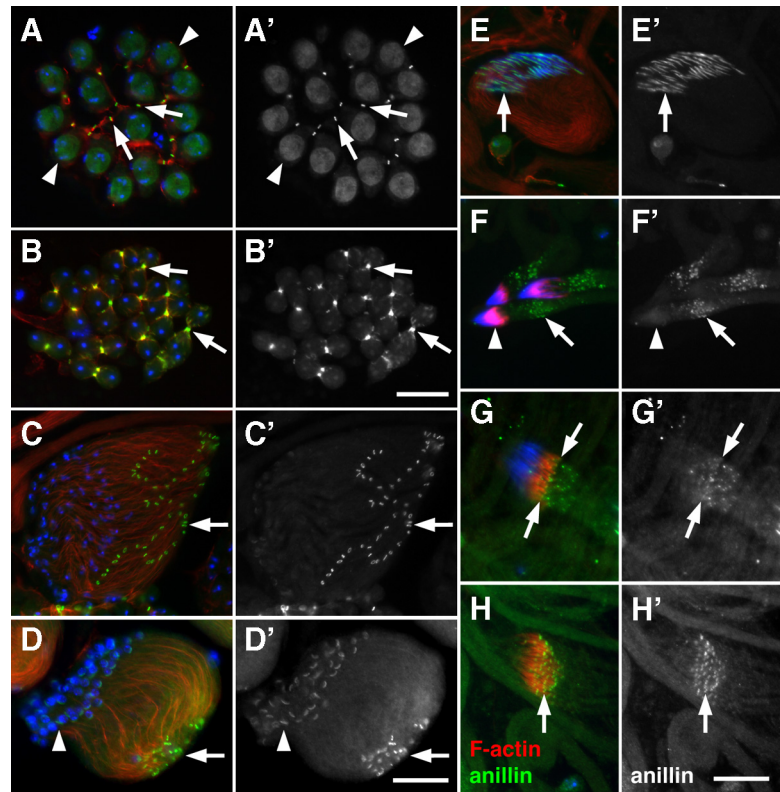


Figure 1. Anillin localizes to actin-rich structures during spermatogenesis. (A–H) Fluorescence micrographs of male germ cells stained for F-actin (red), anillin (green), and DNA (blue) and (A'–H') corresponding grayscale images of anillin alone. (A) Primary spermatocytes with F-actin in the fusome and anillin in mitotic ring canals (arrows) and nuclei (arrowheads). (B) Dividing spermatocytes showing colocalization of F-actin and anillin in the cleavage furrow (arrows). (C) Cyst of 64 early elongating spermatids with anillin in ring canals (arrow). (D) Cyst of elongating spermatids showing a high concentration of F-actin near ring canals (arrow). Anillin and F-actin are also present in the dense body (arrowhead), which forms a crescent along one side of each spermatid nucleus. (E) Group of 64 elongated sperm nuclei. Anillin and actin persist in the dense body (arrow) throughout nuclear shaping. (F) Actin cones forming over three clusters of 64 nuclei. Anillin localizes to puncta (arrow) in the vicinity of the actin cones (arrowhead). (G) Puncta of anillin coalesce at the leading edge of actin cones (arrows) as they prepare to move away from the mature sperm nuclei. (H) Anillin localizes to the leading edge of actin cones (arrow) that have progressed along the length of the cyst. Bars, 20 μm .

expressed in early primary spermatocytes using Bam-GAL4 (Chen and McKearin, 2003; Dietzl *et al.*, 2007). These dsRNAs, which were directed against different portions of the *anillin* gene, also caused formation of multinucleate cells (Figure 2E, and not shown). Because expression of the UAS-dsRNA construct caused a highly penetrant cytokinesis defect, we used this line in subsequent experiments.

To confirm that anillin protein levels were knocked down, we examined dsRNA-expressing male germ cells using anti-anillin antibody. In wild-type spermatocytes, anillin localized to interphase nuclei and to mitotically formed ring canals (Figure 2F). In spermatocytes expressing dsRNA directed against *anillin*, anillin protein levels were greatly reduced in spermatocyte nuclei, but remained in mitotic ring canals, which formed before dsRNA expression (Figure 2G). In meiotically dividing wild-type male germ cells, anillin colocalized with F-actin in the contractile ring (Figure 2H). However, in dsRNA-expressing cells, anillin was absent from the cleavage furrow, and F-actin was either diffusely localized or absent (Figure 2I, and see below). Immunoblotting of whole testis proteins confirmed that anillin levels were greatly reduced in dsRNA-expressing cells (Figure 2J). Thus, RNAi directed against *anillin* depleted anillin protein at postmitotic stages.

To determine if anillin has later functions in spermiogenesis, we examined dsRNA-expressing male germ cells for defects in differentiation and individualization. Loss of anillin had no obvious effect on polarity, elongation, or differentiation of spermatid cysts (not shown). However, actin cone formation appeared somewhat aberrant. In male germ cell cysts expressing dsRNA directed against *anillin*, investment cones exhibited two phenotypes: some appeared thinner than normal and lacked myosin VI (Supplemental Figure S1B), whereas others were short with diffuse myosin VI (Supplemental Figure S1C). Similar investment cone defects

were observed in male germ cells mutant for the phosphatidylinositol 4-kinase *Fwd*, which is also required for cytokinesis (Supplemental Figure S1, D and E), suggesting that failure to make normal investment cones may be a secondary consequence of cytokinesis failure. For this reason, we focused on the role of anillin in meiotic cytokinesis.

Anillin, Septins, and Myosin II Are Stably Associated with the Contractile Ring

For anillin and the septins to provide a stable anchor for the contractile ring, they should remain tightly associated with the cleavage furrow during cytokinesis. To test this idea, we examined GFP fusions to anillin and the septin *Sep2* in FRAP experiments. We also tested a GFP fusion to myosin II regulatory light chain (*Sqh*), which we expected to be more dynamic during cleavage. Using live spermatocytes in fibrin clots (Royou *et al.*, 2002; Wong *et al.*, 2005, 2007), we photobleached one side of the cleavage furrow and measured fluorescence intensity levels in the bleached and unbleached sides over time. As a positive control, we examined the behavior of PLC δ -PH-GFP, a marker for plasma membrane-associated phosphatidylinositol 4,5-bisphosphate (PIP₂; Wong *et al.*, 2005), which recovered rapidly with a $t_{1/2}$ of 6.4 ± 1.3 s (Figure 3, A and E; mean \pm SD; $n = 5$). In contrast, GFP-anillin (GFP-anil), *Sep2*-GFP, and *Sqh*-GFP showed only low levels of recovery even after 5 min. Specifically, GFP-anil reached $37.2 \pm 5.1\%$ (Figure 3, B and F; mean \pm SD; $n = 5$) of initial levels, *Sep2*-GFP reached $20.6 \pm 3.9\%$ (Figure 3, C and G; mean \pm SD; $n = 5$), and *Sqh*-GFP reached $29.5 \pm 8.1\%$ (Figure 3, D and H; mean \pm SD; $n = 4$). These numbers likely overestimate the degree of turnover of GFP-anil, *Sep2*-GFP, and *Sqh*-GFP, because a significant proportion of the observed recovery may be due to unbleached material entering the region of interest during constriction (see also Carvalho *et al.*, 2009). Thus, these data suggest that core

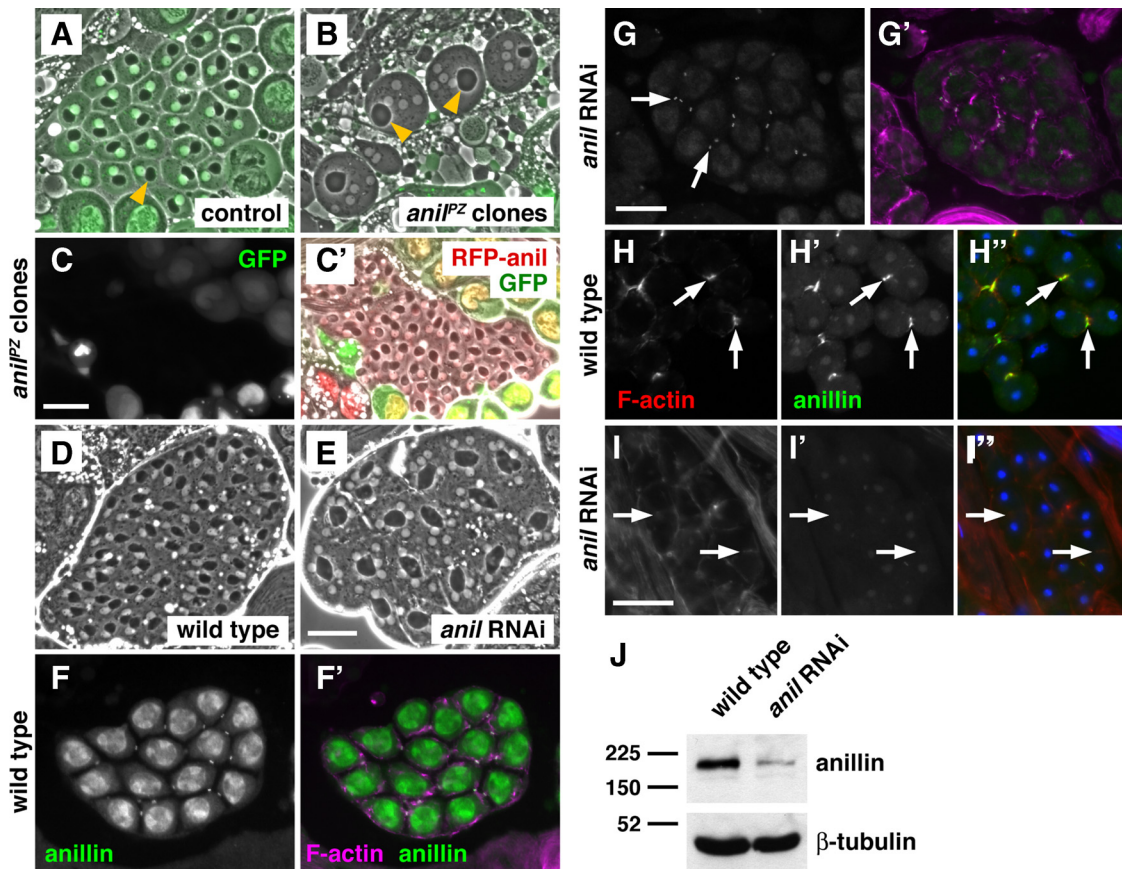


Figure 2. Anillin is required for spermatocyte cytokinesis. (A, B, D, and E) Phase-contrast micrographs of early round spermatids, showing nuclei (white disks) and mitochondrial derivatives (dark organelles). (A and B) Spermatids from testes in which *anillin* mutant (*anil^{PZ}*) clones were generated by FLP-FRT-mediated recombination (see *Materials and Methods*). (A) Wild-type spermatids are marked by nuclear GFP and have one nucleus per mitochondrial derivative (yellow arrowhead). (B) *anillin* mutant spermatids, marked by absence of GFP, contain multiple nuclei and enlarged mitochondrial derivatives (yellow arrowheads), indicating failure of meiotic cytokinesis. (C and C') Expression of mRFP-anillin rescues the cytokinesis defects of *anillin* mutant clones. Fluorescence micrograph (C) of a GFP-negative cyst of rescued, mononucleate early spermatids (C') expressing mRFP-anillin (red). (D and E) Spermatids from wild-type (D) testes and testes in which male germ cells are expressing dsRNA targeted against *anillin* (E). Note that the samples in C–E were not flattened as much as those in A and B. (F and G) Fluorescence micrographs of primary spermatocytes stained for anillin. (F' and G') Corresponding merged images showing anillin (green) and F-actin (magenta). Anillin localizes to nuclei and mitotic ring canals in wild type (F), whereas in dsRNA-expressing cells, anillin is still present in mitotic ring canals, but levels of nuclear anillin protein are greatly reduced (G). (H–H'' and I–I'') Dividing spermatocytes stained for anillin (green), F-actin (red), and DNA (blue). In cleavage furrows (arrows) of wild-type spermatocytes, F-actin (H), and anillin (H') colocalize (H''), whereas in dsRNA-expressing cells F-actin appears diffuse (I), and anillin is absent (I'). Bars, 20 μ m. (J) Immunoblot showing reduced anillin (~190 kDa) levels in dsRNA-expressing male germ cells compared with wild type. β -Tubulin (~50 kDa) is used as a loading control.

components of the cleavage furrow and contractile ring exist in stable rather than dynamic structures during *Drosophila* spermatocyte cytokinesis.

Anillin Recruits Septins and Maintains Rho, F-Actin, and Myosin II at the Cleavage Furrow

Because anillin is known to bind septins, F-actin, myosin II, and Rho, we examined localization of these proteins in dividing spermatocytes depleted for anillin. In wild-type spermatocytes, the septins peanut and Sep2 were concentrated in the cleavage furrow (Figure 4, A and C), whereas septins were absent from the cleavage furrow in male germ cells expressing dsRNA directed against *anillin* (Figure 4, B and D). F-actin was recruited to the cleavage furrow in anillin-depleted spermatocytes, but its localization appeared diffuse, especially at late stages of cytokinesis (cf. Figure 4 A' and B'). Rho localization also appeared defective in dividing spermatocytes lacking anillin. Anillin colocalized with Rho at the cleavage furrow in

wild-type cells (Figure 4E). However, in male germ cells depleted for anillin, the small amount of Rho detected at the cleavage furrow appeared diffuse (Figure 4F).

To determine whether anillin is required to restrict myosin II to the equator of dividing spermatocytes, we examined live cells embedded in fibrin clots for localization of Sqh-GFP. In wild-type cells, Sqh-GFP was concentrated in the cleavage furrow during all stages of constriction (Figure 4G and Supplemental Video 1; $n = 3/3$ cells). Sqh-GFP was no longer restricted to the equator in spermatocytes depleted of anillin. Rather, Sqh-GFP appeared to move around the periphery of the cell during cleavage (Figure 4H and Supplemental Video 2; $n = 5/6$ cells). In addition, the membranes of dividing anillin-depleted cells exhibited blebbing and undulations not observed in wild type. Thus, anillin is required for localization of septins and also for maintenance of Rho, F-actin, and myosin II, at the cleavage furrow in dividing *Drosophila* spermatocytes.

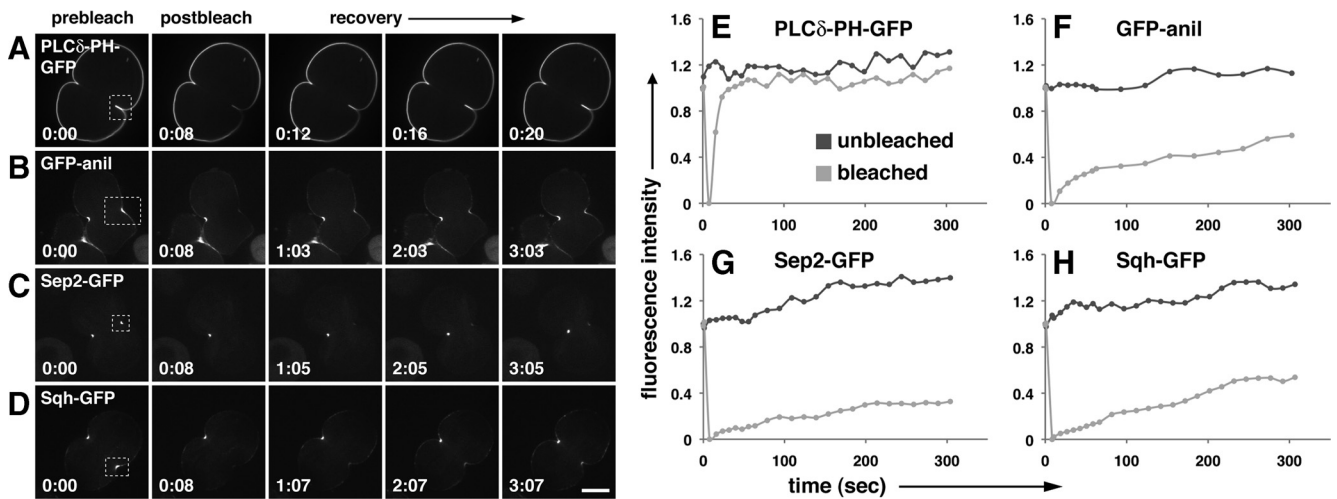
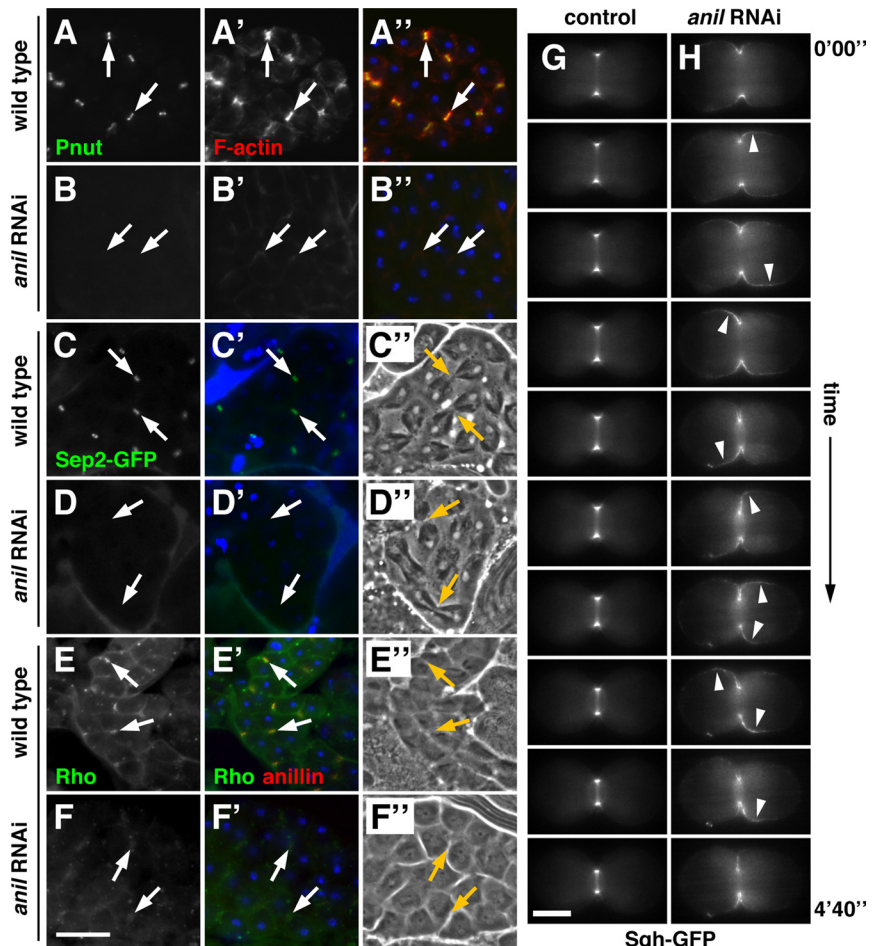


Figure 3. Anillin, septins, and myosin II are stably associated with the cleavage furrow. Fluorescence micrographs (A–D) and corresponding graphs of dividing spermatocytes examined for FRAP (E–H). (A–D) Micrographs show cells before bleaching (prebleach), immediately after bleaching (postbleach), and during recovery. The bleached area is shown (box with dotted lines). Times are in minutes:seconds. (E–H) Graphs show recovery of fluorescence in bleached area versus control (unbleached). Fluorescence intensity is indicated relative to starting intensity, which was set at 1. Time is in seconds. (A and E) PLC δ -PH-GFP, which associates with plasma membrane PIP₂, recovers rapidly after photobleaching, whereas GFP-anillin (B and F), Sep2-GFP (C and G), and Sqh-GFP (D and H) fail to recover even after 5 min. Bar, 10 μ m.

To further examine Sqh-GFP behavior in anillin-depleted cells, we performed FRAP on spermatocytes coexpressing

Sqh-GFP and dsRNA targeted against *anillin* (Figure 5). In these cells, the bleached side of the furrow recovered at a

Figure 4. Anillin is required for recruitment of septins and stabilization of Rho and myosin II at the cleavage furrow. (A–A'' and B–B'') Dividing spermatocytes stained for the septin peanut (Pnut; green), F-actin (red), and DNA (blue). In cleavage furrows (arrows) of wild-type spermatocytes, peanut (A) and F-actin (A') colocalize in cleavage furrows (A''), whereas in dsRNA-expressing cells peanut is absent (B) and F-actin appears diffuse (B'). (C–D') Dividing spermatocytes expressing Sep2-GFP (green) and stained for DNA (blue) with corresponding phase-contrast micrographs (C'' and D''). Sep2-GFP localizes to cleavage furrows in wild-type cells (C), but is absent in dsRNA-expressing cells (D). (E–F') Dividing spermatocytes stained for Rho (green), anillin (red), and DNA (blue) with corresponding phase-contrast micrographs (E'' and F''). In cleavage furrows of wild-type spermatocytes, Rho (E) and anillin colocalize in cleavage furrows (E''), whereas in dsRNA-expressing cells Rho appears diffuse (F) and anillin is absent (F'). Bar, 20 μ m. (G and H) Time-lapse images showing the change in localization of Sqh-GFP (myosin regulatory light chain) during cytokinesis. In control cells, Sqh-GFP is tightly associated with the furrow (G), whereas in dsRNA-expressing cells Sqh-GFP moves around the cell cortex in an oscillatory manner (H). The images shown were taken at 40-s intervals. Corresponding full-length videos are available online (Supplemental Videos 1 and 2). Bar, 5 μ m.



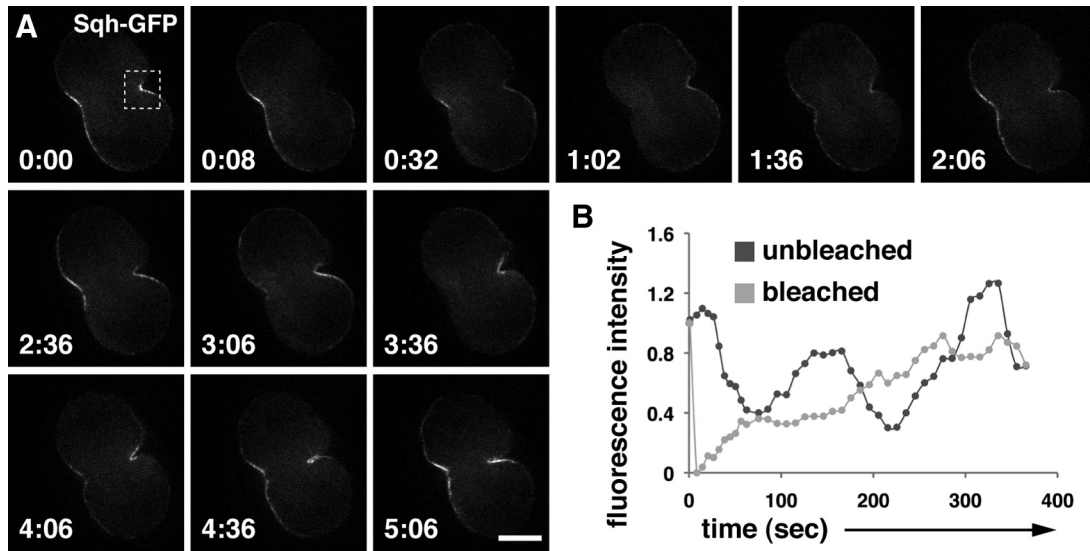


Figure 5. Anillin is required for tight association of myosin II with the cleavage furrow. Fluorescence micrograph (A) and corresponding graph (B) of a dividing spermatocyte, expressing Sqh-GFP and dsRNA directed against *anillin*, examined for FRAP. (A) Micrograph showing cell before bleaching, immediately after bleaching, and during recovery. The bleached area is shown (box with dotted lines). Times are in minutes:seconds. (B) Graph showing recovery of fluorescence in bleached area versus control (unbleached). Fluorescence intensity is indicated relative to starting intensity, which was set at 1. (A and B) Fluorescence intensity increases and decreases in both bleached and unbleached areas as Sqh-GFP flows in and out of the furrow region. Time is in seconds. Bar, 10 μ m.

greater rate and to a greater extent than in control cells (cf. Figure 5, A and B, with Figure 3, D and H). Specifically, fluorescence intensity in the bleached region recovered to more than 90% of its original value after 185 ± 54.5 s (mean \pm SD, $n = 5/6$ cells). Meaningful half times of recovery could not be calculated because fluorescence recovery was not related to standardized rates of GFP molecule diffusion. Instead, delocalized Sqh-GFP flowed in and out of the furrow region, causing the bleached and unbleached sides of the furrow to be indistinguishable after a short period of time. Thus, anillin is essential for persistent association of myosin with the furrow membrane.

Loss of Anillin Is Suppressed by Expression of DE-Cadherin

Because loss of anillin affects late telophase, a stage of cytokinesis when membrane trafficking is required, we tested the requirement for anillin in localization of several membrane-trafficking markers. In early wild-type dividing spermatocytes, a GFP fusion to *Drosophila* E-cadherin (DE-cad-GFP) localized to the cell cortex and to puncta at the poles of the cells (Figure 6A). By mid-cytokinesis, DE-cad-GFP was found in puncta at the poles of the cells and also started to accumulate in puncta at the equator (Figure 6B). In late

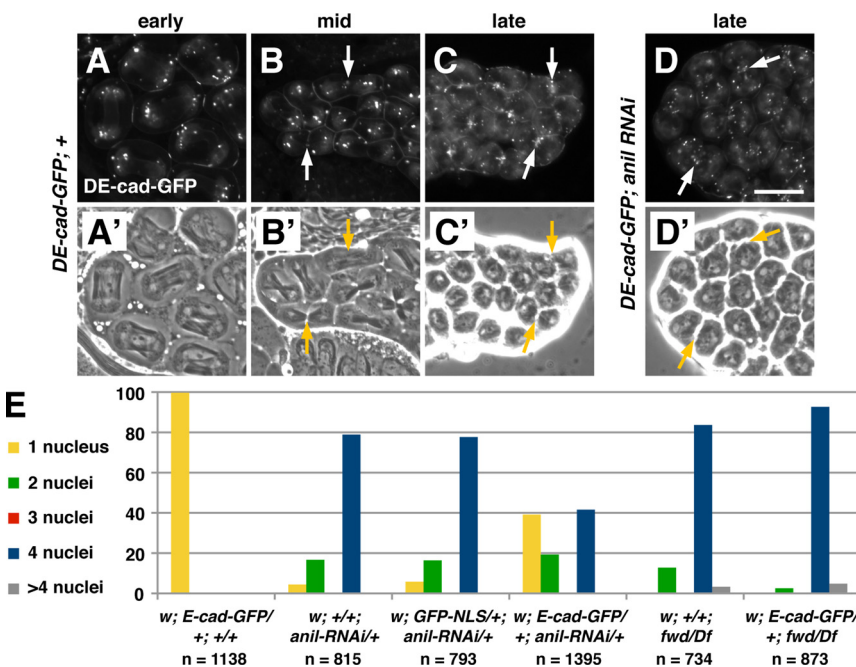


Figure 6. DE-cad-GFP suppresses cytokinesis defects caused by *anillin* depletion. (A–D') Fluorescence (A–D) and corresponding phase-contrast (A'–D') micrographs of dividing spermatocytes expressing DE-cad-GFP. (A and A') In wild-type cells DE-cad-GFP localizes to the cortex and in puncta at the poles during anaphase. During telophase, DE-cad-GFP begins to accumulate at the equator (arrows; B and B'). By late telophase, DE-cad-GFP becomes highly concentrated in the furrow in wild-type (C and C') and dsRNA-expressing cells (D and D'). (E) Expression of DE-cad-GFP greatly reduces the percentage of multinucleate spermatids in flies expressing dsRNA directed against *anillin* but not in flies mutant for *fwd*. The number of spermatids counted for each genotype is indicated (n). Note that although these results were obtained with the UAS:*anillin-RNAi* line, similar results were obtained for β_2 ::*anillin-RNAi* (not shown; see Materials and Methods). Bar, 20 μ m.

telophase, puncta of DE-cad-GFP were highly concentrated at the equator of dividing cells (Figure 6C). DE-cad-GFP localization appeared normal in spermatocytes depleted for anillin (Figure 6D). Similarly, in both wild-type and anillin-depleted spermatocytes, a GFP fusion to clathrin light chain (CLC-GFP) and a secreted GFP marker (sGFP) localized to the equator of dividing cells (Supplemental Figure S2, A–D). These data suggest that anillin does not play an important role in membrane trafficking to the cleavage furrow.

Remarkably, we found that expression of DE-cad-GFP, but not CLC-GFP or sGFP, had an unanticipated effect on cytokinesis in anillin-depleted cells. Male germ cells coexpressing DE-cad-GFP and dsRNA directed against *anillin* had an increased frequency of successful cytokinesis, relative to cells expressing dsRNA alone (Figure 6E). In wild type, 99.6% of spermatids were mononucleate, indicating successful meiotic cytokinesis. In contrast, only 4.4% of spermatids depleted of anillin were mononucleate, and 16.7% of anillin-depleted spermatids had two nuclei per cell, indicating failure of cytokinesis during meiosis I or meiosis II; 78.9% of spermatids had four nuclei per cell, indicating cytokinesis failure during both meiosis I and II. Expression of a nuclear GFP marker had no effect on spermatids depleted of anillin. However, ubiquitous expression of DE-cad-GFP resulted in significant suppression of the cytokinesis defect caused by anillin loss: 39.1% of spermatids were mononucleate, 19.3% were binucleate, and 41.6% had four nuclei. Suppression of the cytokinesis defect by DE-cad-GFP was specific to anillin, as DE-cad-GFP had no effect on cytokinesis failures due to loss of *fwd* (Figure 6E). Thus, expression of DE-cad partially bypasses the requirement for anillin during cytokinesis.

Adherens Junction Proteins Can Substitute for Anillin in Anchoring F-Actin at the Cleavage Furrow

Because expression of DE-cad-GFP suppressed loss of anillin, we asked whether DE-cad and other members of the cadherin–catenin complex are normally expressed in developing male germ cells. Immunofluorescence experiments using specific antisera revealed that β -catenin (armadillo), α -catenin, and DE-cad are normally undetectable in dividing spermatocytes (Figure 7, A and B; Supplemental Figure S3, C and F), whereas all three proteins were present in somatic structures found in the same preparations (Supplemental Figure S3, A, B, D, and E; α -catenin not shown). Strikingly, expression of DE-cad-GFP resulted in recruitment of armadillo and α -catenin to membrane structures including cleavage furrows of dividing cells (Figure 7, C and D). In addition, Western blot analysis revealed increased armadillo and α -catenin protein levels in DE-cad-GFP-expressing cells compared with wild type (Supplemental Figure S4). Thus, DE-cad expression appears to stabilize and localize endogenous adherens junction proteins in dividing spermatocytes.

To determine if DE-cad-GFP expression suppresses loss of anillin by retaining F-actin at the cell equator, we examined F-actin localization in live cells using an mCherry fusion to the F-actin-binding calponin-homology domain of utrophin (mCherry-Utr-CH; Burkel *et al.*, 2007). During cleavage in wild-type and DE-cad-GFP-expressing cells, F-actin remained highly concentrated at the equator of the cell (Figure 8, A and B; Supplemental Videos 3 and 4, $n = 5/6$ cells for wild type and $n = 4/5$ cells for DE-cad-GFP). In contrast, in anillin-depleted cells, F-actin moved around the cell cortex, similar to the behavior of myosin II. We observed different levels of phenotypic severity: cells were characterized as normal when localization of F-actin resembled controls, intermediate where there was some movement of F-actin from

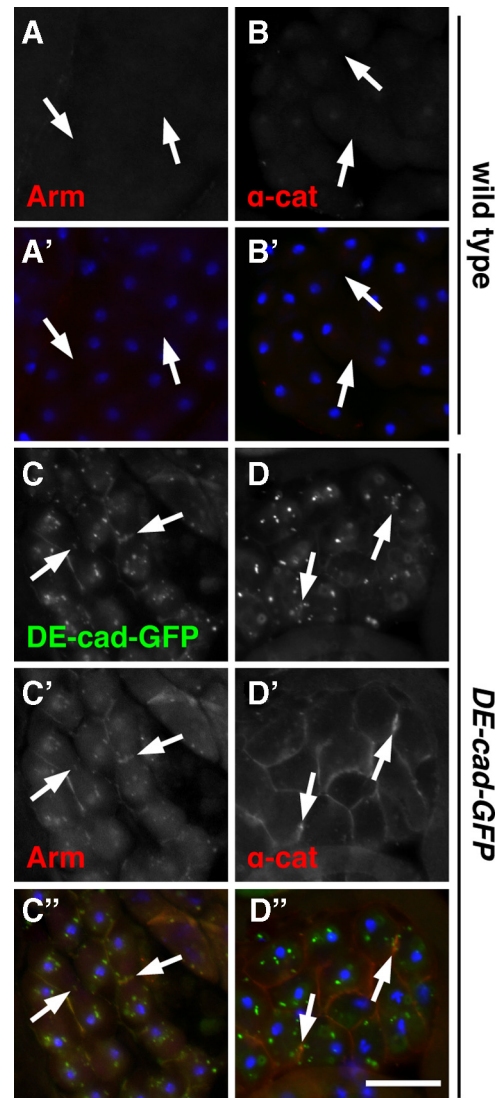


Figure 7. DE-cad-GFP recruits armadillo and α -catenin to the cleavage furrow. Fluorescence micrographs of dividing wild-type (A–A' and B–B') or DE-cad-GFP-expressing (C–C' and D–D') spermatocytes stained for armadillo (Arm) or α -catenin (α -cat). In wild type, Arm (A) and α -cat (B) are absent from the cleavage furrow (arrows). However, in cells expressing DE-cad-GFP (C and D), Arm (C') and α -cat (D') are clearly recruited to the furrow and to other regions of the plasma membrane. Arm also colocalizes with DE-cad in intracellular puncta. (A', B', C', and D'') Corresponding merged images showing DE-cad-GFP (green, C'' and D''), Arm (red, A' and C''), α -cat (red, B' and D'') and DNA (blue). Bar, 20 μ m.

pole to pole, or severe when oscillations were dramatic and accompanied by the majority of F-actin leaving the area of the furrow. Of cells expressing dsRNA directed against anillin, none of the cells were normal, 2/7 were intermediate and 5/7 were severe (Figure 8C and Supplemental Video 5). In contrast, of cells depleted of anillin and expressing DE-cad-GFP, 1/7 were normal, 6/7 were intermediate (Figure 8D and Supplemental Video 6), and none were severe. Thus, like anillin, adherens junction proteins can restrict actomyosin contractility to the equator of the cell.

To determine if DE-cad-GFP substitutes for anillin by recruiting septins to the cleavage furrow, we examined peanut localization in anillin-depleted cells expressing DE-cad-

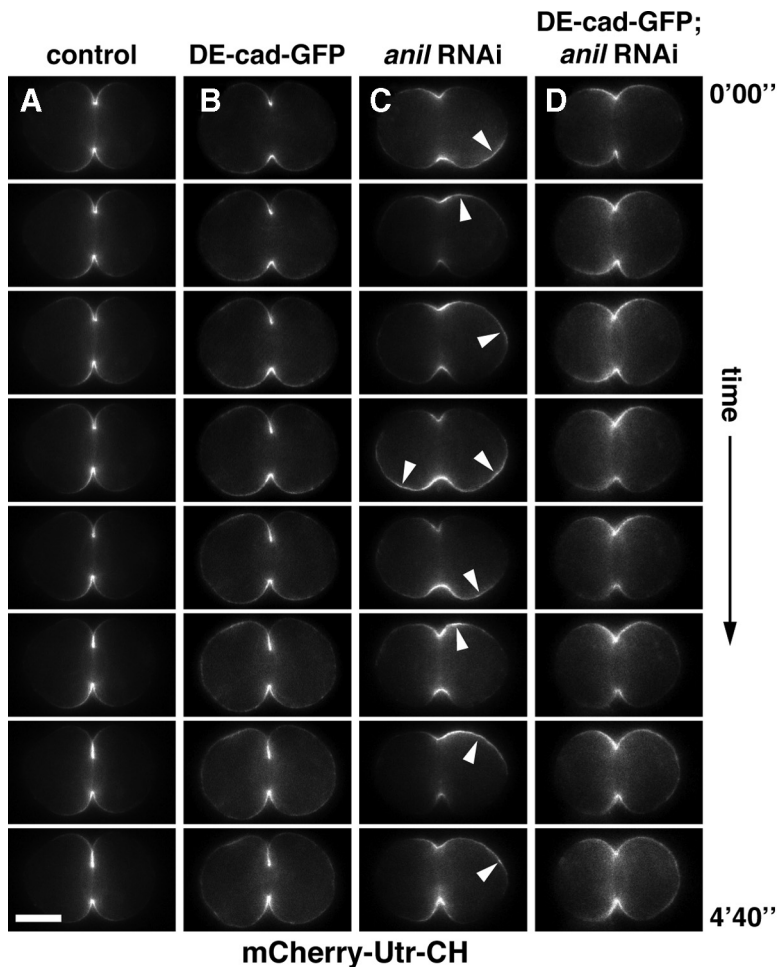


Figure 8. Anillin and DE-cadherin restrict F-actin to the cleavage furrow. (A–D) Time-lapse images showing the change in localization of mCherry-Utr-CH (which binds F-actin) during spermatocyte cytokinesis. In control cells (A) and cells expressing DE-cad-GFP (B), mCherry-Utr-CH is tightly associated with the furrow, whereas in dsRNA-expressing cells mCherry-Utr-CH moves around the cell cortex in an oscillatory manner (C). DE-cad-GFP expression stabilizes mCherry-Utr-CH at the furrow in anillin-depleted cells (D). The images shown were taken at 40-s intervals. Corresponding full-length videos are available online (Supplemental Videos 3–6). Bar, 5 μ m.

GFP. Unlike wild-type cells, in which peanut was abundant at the cell equator (Supplemental Figure S5A), cells expressing dsRNA directed against *anillin* had no detectable peanut at the equator regardless of whether DE-cad-GFP was coexpressed (Supplemental Figure S5, B and C). Thus, our data suggest that DE-cad-GFP promotes successful cytokinesis by providing an alternative means of anchoring F-actin and myosin at the cleavage furrow.

Expression of E-Cadherin Restores Cytokinesis to Mouse Fibroblasts Depleted of Anillin

To test whether classic cadherins are generally capable of suppressing loss of anillin function, we examined mouse L-fibroblast cells expressing E-cadherin (E-cad) under control of an inducible promoter (Angres *et al.*, 1996). Knockdown of anillin with two different shRNAs caused a cytokinesis defect in cells grown in the absence of E-cad induction, resulting in 43 or 47% multinucleate cells (Figure 9 and not shown). In contrast, expression of E-cad substantially suppressed the cytokinesis defect caused by anillin depletion, resulting in only 24 or 22% polyploidy (Figure 9 and not shown). Thus, E-cad expression is sufficient to render mammalian cells less sensitive to loss of anillin.

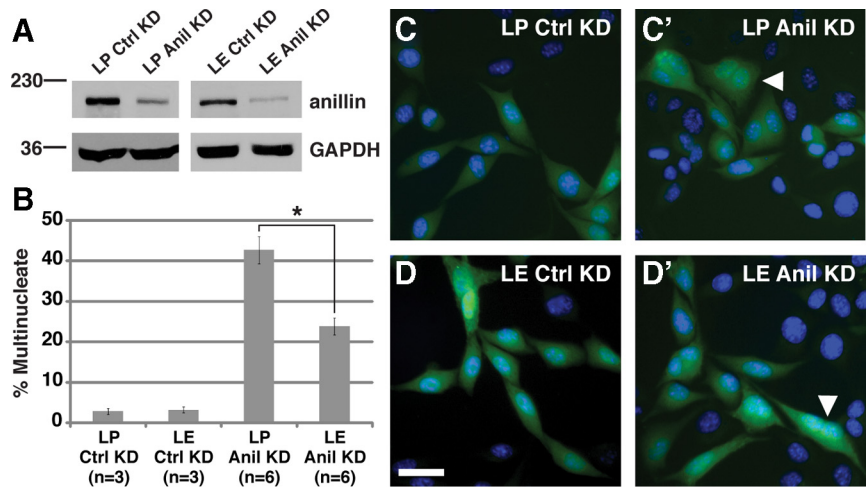
DISCUSSION

Successful cytokinesis requires anchoring of the contractile ring to the plasma membrane in the plane of division. An-

illin has been postulated to play this role by recruiting septins and binding and stabilizing F-actin and myosin II during animal cell cytokinesis (reviewed in Eggert *et al.*, 2006). Our results are consistent with this model and show for the first time that anillin is required to restrict F-actin to the equator. Moreover, we find that anillin and the septins can be replaced by the cadherin–catenin complex to carry out this critical function. The interchangeability of these nonhomologous cassettes suggests that two shared properties are required during cytokinesis: the ability to form a stable attachment to the plasma membrane and the ability to bind and bundle actin filaments.

Based on our FRAP results, as well as those from worms (Carvalho *et al.*, 2009) and yeast (Berlin *et al.*, 2003; Dobbelaere *et al.*, 2003; Clifford *et al.*, 2008), anillin and the septins are stably associated with the cleavage furrow and do not undergo rapid exchange during constriction of the contractile ring. Tight linkage of these proteins to the furrow membrane is likely mediated, at least in part, by septins. Septins bind phosphoinositides *in vitro*, and their localization is affected by alterations in phosphoinositide levels *in vivo* (Zhang *et al.*, 1999; Casamayor and Snyder, 2003; Rodriguez-Escudero *et al.*, 2005; Kouranti *et al.*, 2006; Tanaka-Takiguchi *et al.*, 2009; our unpublished results). Because plasma membrane-associated septin filaments form a gauze-like mesh that serves as a diffusion barrier (Takizawa *et al.*, 2000; Schmidt and Nichols, 2004; Finger, 2005; Rodal *et al.*, 2005), binding of septins to PIP₂-containing membranes

Figure 9. Expression of E-cadherin suppresses cytokinesis defects caused by depletion of *anillin* in mouse L-cells. (A) Immunoblots showing reduced levels of anillin protein (~190 kDa) in anillin shRNA-expressing mouse LP (empty vector) or LE (E-cadherin expressing) cells (Anil KD) compared with scrambled shRNA-expressing cells (Ctrl KD). GAPDH (~40 kDa) is the loading control. (B) Quantitation of multinucleate cells confirms suppression of anillin loss by expression of E-cadherin. * $p = 0.00076$. n is the number of experiments, and 100 cells were counted in triplicate for each experiment. (C and D) Micrographs of LP and LE cells expressing scrambled shRNA (C and D) or anillin shRNA (C' and D') marked by GFP (green). DNA is stained with Hoechst (blue). Representative multinucleate cells are marked (white arrowheads). Bar, 100 μm .



in the cleavage furrow likely promotes formation of a stable molecular fence. Although anillin has not been shown to bind phospholipids directly, the presence of a conserved pleckstrin homology domain (Oegema *et al.*, 2000) suggests that anillin may also interact with membranes. Indeed, in septin knockdown cells, anillin localizes to the membrane in a Rho-dependent manner (Straight *et al.*, 2005; Hickson and O'Farrell, 2008; Piekny and Glotzer, 2008).

Anillin binds and bundles actin filaments and also binds myosin II, thereby interacting directly with both major components of the contractile ring (Field and Alberts, 1995; Straight *et al.*, 2005). Our data and those of Carvalho *et al.* (2009) suggest for the first time that filaments of myosin II and actin, like anillin and the septins, do not turn over in the cleavage furrow, but rather are disassembled during constriction. We therefore propose that anillin stabilizes the cleavage furrow by linking the actomyosin ring to septin filaments on the membrane. Consistent with this, loss of anillin leads to destabilization of myosin II and F-actin, which move freely around the plasma membrane during cleavage of anillin-deficient cells (Straight *et al.*, 2005; Hickson and O'Farrell, 2008; Piekny and Glotzer, 2008; our results). Indeed, our FRAP data confirm that myosin completely loses its stable association with the furrow in anillin-depleted cells. Anillin may also stabilize the contractile ring through indirect interactions with microtubule plus ends at the cell equator (D'Avino *et al.*, 2008; Gregory *et al.*, 2008; Hickson and O'Farrell, 2008). However, our data suggest that the membrane-actin cross-linking properties of anillin and the cadherin-catenin complex may be sufficient to promote cytokinesis.

Expression of DE-cad partially restores cytokinesis to anillin-depleted spermatocytes, indicating that the cadherin-catenin complex, like the anillin-septin cassette, is capable of linking the actomyosin ring to the furrow membrane. Classic cadherins such as DE-cad are transmembrane proteins that form stable membrane attachments by virtue of their ability to mediate cell-cell adhesion (Takeichi, 1995). Ectopically expressed fluorescent E-cadherin and DE-cad fusion proteins localize to the cleavage furrow, where they associate with β -catenin (armadillo) and α -catenin during cytokinesis (Bauer *et al.*, 2008; our results). Homodimers of α -catenin bind and bundle actin filaments (Weis and Nelson, 2006; Hartsock and Nelson, 2008), suggesting that α -catenin is ideally suited to substitute for anillin during cytokinesis. Importantly, we found that expression of E-cad in mouse L-cells renders them less sensitive to loss of anillin, supporting this idea. Indeed, our finding that DE-cad and E-cad behave simi-

larly in this respect suggests that cells expressing adherens junction proteins may be less sensitive to loss of anillin during animal development. Our data show that classic cadherins can stabilize F-actin in the contractile ring. Adherens junctions can also tether minus ends of microtubules (Meng *et al.*, 2008), but whether they can associate with and stabilize microtubule plus ends in the furrow remains unknown.

Our results suggest cells may exhibit differential sensitivity to loss of anillin *in vivo*, depending on the presence of alternative mechanisms to link F-actin and myosin to the plasma membrane. Ezrin/radixin/moesin proteins are cytoskeletal-membrane cross-linkers that localize to the cleavage furrow and could potentially carry out this function (Sato *et al.*, 1991; Carreno *et al.*, 2008; Kunda *et al.*, 2008). In any case, it is likely that DE-cad-mediated suppression of the cytokinesis defects in anillin-depleted cells relies on a small amount of residual anillin and septins, because presumably these proteins are required for stabilization of postdivision ring canals.

Our experiments raise the question of whether cadherin-mediated cell-cell adhesion is normally important for cytokinesis. Indeed, only a few studies suggest a link between cadherins and cell cleavage. In the early zebrafish embryo, daughter blastomeres transition from being loosely associated to having tightly apposed membranes. This is accomplished after ingress via delivery of adhesion proteins including E-cadherin and β -catenin to newly formed daughter membranes (Jesuthasan, 1998; Li *et al.*, 2006). Disruption of cadherin-mediated adhesion causes defects in blastomere cohesion, but not in cytokinesis (Jesuthasan, 1998). In mouse fibroblasts, the introduction of E-cadherin- α -catenin fusion proteins has the opposite effect, causing a slight inhibition of cytokinesis (Nagafuchi *et al.*, 1994). Because these fusion proteins likely form unregulated junctions that prevent the cells from rounding up during division, cells must coordinate the disassembly of adherens junctions with cytokinesis. Hence, the cadherin-catenin complex may not be required for cytokinesis *per se*, but is involved in changes in tissue architecture that must be tightly linked with cytokinesis.

Anillin may have additional roles beyond cytokinesis *in vivo*. However, it is difficult to obtain cells entirely lacking anillin protein, and earlier defects in cytokinesis may obscure later phenotypes. For example, although we observed defects in actin cone formation in anillin-depleted spermatids, this could reflect either a specific role for anillin in individualization or an indirect effect of cytokinesis failure on membrane topology. Thus, to study anillin function at other stages of development, it will be necessary to identify

temperature-sensitive alleles or employ other techniques to destabilize the anillin protein dynamically in living cells. Interestingly, in a report linking increased anillin expression levels and the progression of diverse human tumors, anillin was highly expressed in both diseased and normal CNS tissues, and similar expression profiles were reported for specific human septins (Hall *et al.*, 2005a,b). Future studies using such techniques may thus uncover exciting new roles for anillin and the septins in the CNS.

ACKNOWLEDGMENTS

We are grateful to Angela Barth, Howard Lipshitz, Ulrich Tepass, Andrew Wilde, and members of the Brill lab for helpful discussions; Anya Cyprys, Tony Harris, Gilles Hickson, and Ulrich Tepass for comments on the manuscript; Henry Chang, Karen Hales, Roger Karess, Hiroki Oda, Ulrich Tepass, and the Bloomington *Drosophila* stock center for fly stocks; Christine Field, Kathryn Miller, Ulrich Tepass, and the Developmental Studies Hybridoma Bank for antibodies; William Bement, Brian Burkel, Helmut Krämer, Erik Snapp, Roger Tsien, and the Canadian *Drosophila* Microarray Centre for plasmids; James Nelson for mouse L-cells; and Paul Paroutis (The Hospital for Sick Children Imaging Facility) for help with FRAP experiments. This work was funded by a University of Toronto Open Scholarship (P.G.), an Ontario Graduate Scholarship, CIHR CGS Scholarship (N.B.), and The Hospital for Sick Children Restrcomp funding (R.W.), and grants from the Terry Fox Foundation (National Cancer Institute of Canada Grant 16425 (J.A.B.)), the Canadian Cancer Society Research Institute Grant 17376 9 (W.S.T.), and the Canadian Institutes of Health Research Grant IG1-93477 (J.A.B.).

REFERENCES

Angres, B., Barth, A., and Nelson, W. (1996). Mechanism for transition from initial to stable cell-cell adhesion: kinetic analysis of E-cadherin-mediated adhesion using a quantitative adhesion assay. *J. Cell Biol.* *134*, 549–557.

Ashburner, M. (1990). *Drosophila: A Laboratory Handbook*, Cold Spring Harbor, NY: Cold Spring Harbor Press.

Bauer, T., Motosugi, N., Miura, K., Sabe, H., and Hiiragi, T. (2008). Dynamic rearrangement of surface proteins is essential for cytokinesis. *Genesis* *46*, 152–162.

Berlin, A., Paoletti, A., and Chang, F. (2003). Mid2p stabilizes septin rings during cytokinesis in fission yeast. *J. Cell Biol.* *160*, 1083–1092.

Brill, J. A., Hime, G. R., Scharer-Schuks, M., and Fuller, M. T. (2000). A phospholipid kinase regulates actin organization and intercellular bridge formation during germline cytokinesis. *Development* *127*, 3855–3864.

Burkel, B. M., von Dassow, G., and Bement, W. M. (2007). Versatile fluorescent probes for actin filaments based on the actin-binding domain of utrophin. *Cell Motil. Cytoskelet.* *64*, 822–832.

Campbell, R. E., Tour, O., Palmer, A. E., Steinbach, P. A., Baird, G. S., Zacharias, D. A., and Tsien, R. Y. (2002). A monomeric red fluorescent protein. *Proc. Natl. Acad. Sci. USA* *99*, 7877–7882.

Carreno, S., Kouranti, I., Glusman, E. S., Fuller, M. T., Echard, A., and Payre, F. (2008). Moesin and its activating kinase Slik are required for cortical stability and microtubule organization in mitotic cells. *J. Cell Biol.* *180*, 739–746.

Carvalho, A., Desai, A., and Oegema, K. (2009). Structural memory in the contractile ring makes the duration of cytokinesis independent of cell size. *Cell* *137*, 926–937.

Casal, J., Gonzalez, C., and Ripoll, P. (1990). Spindles and centrosomes during male meiosis in *Drosophila melanogaster*. *Eur. J. Cell Biol.* *51*, 38–44.

Casamayor, A., and Snyder, M. (2003). Molecular dissection of a yeast septin: distinct domains are required for septin interaction, localization, and function. *Mol. Cell. Biol.* *23*, 2762–2777.

Chang, F., Woollard, A., and Nurse, P. (1996). Isolation and characterization of fission yeast mutants defective in the assembly and placement of the contractile actin ring. *J. Cell Sci.* *109*(Pt 1), 131–142.

Chen, D., and McKearin, D. M. (2003). A discrete transcriptional silencer in the bam gene determines asymmetric division of the *Drosophila* germline stem cell. *Development* *130*, 1159–1170.

Clifford, D. M., Wolfe, B. A., Roberts-Galbraith, R. H., McDonald, W. H., Yates, J. R., 3rd, and Gould, K. L. (2008). The Clp1/Cdc14 phosphatase contributes to the robustness of cytokinesis by association with anillin-related Mid1. *J. Cell Biol.* *181*, 79–88.

D'Avino, P. P. (2009). How to scaffold the contractile ring for a safe cytokinesis—lessons from Anillin-related proteins. *J. Cell Sci.* *122*, 1071–1079.

D'Avino, P. P., Takeda, T., Capalbo, L., Zhang, W., Lilley, K. S., Laue, E. D., and Glover, D. M. (2008). Interaction between Anillin and RacGAP50C connects the actomyosin contractile ring with spindle microtubules at the cell division site. *J. Cell Sci.* *121*, 1151–1158.

Dietzl, G., *et al.* (2007). A genome-wide transgenic RNAi library for conditional gene inactivation in *Drosophila*. *Nature* *448*, 151–156.

Dobbelaere, J., Gentry, M. S., Hallberg, R. L., and Barral, Y. (2003). Phosphorylation-dependent regulation of septin dynamics during the cell cycle. *Dev. Cell* *4*, 345–357.

Doberstein, S. K., Fetter, R. D., Mehta, A. Y., and Goodman, C. S. (1997). Genetic analysis of myoblast fusion: *blown fuse* is required for progression beyond the prefusion complex. *J. Cell Biol.* *136*, 1249–1261.

Echard, A., Hickson, G. R., Foley, E., and O'Farrell, P. H. (2004). Terminal cytokinesis events uncovered after an RNAi screen. *Curr. Biol.* *14*, 1685–1693.

Eggert, U. S., Mitchison, T. J., and Field, C. M. (2006). Animal cytokinesis: from parts list to mechanisms. *Annu. Rev. Biochem.* *75*, 543–566.

Fabrizio, J. J., Hime, G., Lemmon, S. K., and Bazinet, C. (1998). Genetic dissection of sperm individualization in *Drosophila melanogaster*. *Development* *125*, 1833–1843.

Field, C. M., and Alberts, B. M. (1995). Anillin, a contractile ring protein that cycles from the nucleus to the cell cortex. *J. Cell Biol.* *131*, 165–178.

Field, C. M., Coughlin, M., Doberstein, S., Marty, T., and Sullivan, W. (2005). Characterization of *anillin* mutants reveals essential roles in septin localization and plasma membrane integrity. *Development* *132*, 2849–2860.

Finger, F. P. (2005). Reining in cytokinesis with a septin corral. *Bioessays* *27*, 5–8.

Fuller, M. T. (1993). Spermatogenesis. In: *The Development of Drosophila melanogaster*, ed. M. Bate and A. Martinez-Arias, Cold Spring Harbor, NY: Cold Spring Harbor Laboratory Press, 71–147.

Giansanti, M. G., Bonaccorsi, S., Bucciarelli, E., and Gatti, M. (2001). *Drosophila* male meiosis as a model system for the study of cytokinesis in animal cells. *Cell Struct. Funct.* *26*, 609–617.

Giansanti, M. G., Bonaccorsi, S., and Gatti, M. (1999). The role of anillin in meiotic cytokinesis of *Drosophila* males. *J. Cell Sci.* *112*(Pt 14), 2323–2334.

Gregory, S. L., Ebrahimi, S., Milverton, J., Jones, W. M., Bejsovec, A., and Saint, R. (2008). Cell division requires a direct link between microtubule-bound RacGAP and Anillin in the contractile ring. *Curr. Biol.* *18*, 25–29.

Hall, P. A., Jung, K., Hillan, K. J., and Russell, S. E. (2005a). Expression profiling the human septin gene family. *J. Pathol.* *206*, 269–278.

Hall, P. A., Todd, C. B., Hyland, P. L., McDade, S. S., Grabsch, H., Dattani, M., Hillan, K. J., and Russell, S. E. (2005b). The septin-binding protein anillin is overexpressed in diverse human tumors. *Clin. Cancer Res.* *11*, 6780–6786.

Hartsock, A., and Nelson, W. J. (2008). Adherens and tight junctions: structure, function and connections to the actin cytoskeleton. *Biochim. Biophys. Acta* *1778*, 660–669.

Hicks, J. L., Deng, W. M., Rogat, A. D., Miller, K. G., and Bownes, M. (1999). Class VI unconventional myosin is required for spermatogenesis in *Drosophila*. *Mol. Biol. Cell* *10*, 4341–4353.

Hickson, G. R., and O'Farrell, P. H. (2008). Rho-dependent control of anillin behavior during cytokinesis. *J. Cell Biol.* *180*, 285–294.

Hime, G. R., Brill, J. A., and Fuller, M. T. (1996). Assembly of ring canals in the male germ line from structural components of the contractile ring. *J. Cell Sci.* *109*, 2779–2788.

Hoyle, H. D., and Raff, E. C. (1990). Two *Drosophila* beta tubulin isoforms are not functionally equivalent. *J. Cell Biol.* *111*, 1009–1026.

Jesuthasan, S. (1998). Furrow-associated microtubule arrays are required for the cohesion of zebrafish blastomeres following cytokinesis. *J. Cell Sci.* *111*, 3695–3703.

Joo, E., Surka, M. C., and Trimble, W. S. (2007). Mammalian SEPT2 is required for scaffolding nonmuscle myosin II and its kinases. *Dev. Cell* *13*, 677–690.

Kalidas, S., and Smith, D. P. (2002). Novel genomic cDNA hybrids produce effective RNA interference in adult *Drosophila*. *Neuron* *33*, 177–184.

Kellerman, K. A., and Miller, K. G. (1992). An unconventional myosin heavy chain gene from *Drosophila melanogaster*. *J. Cell Biol.* *119*, 823–834.

Kinoshita, M., Field, C. M., Coughlin, M. L., Straight, A. F., and Mitchison, T. J. (2002). Self- and actin-templated assembly of mammalian septins. *Dev. Cell* *3*, 791–802.

Kouranti, I., Sachse, M., Arouche, N., Goud, B., and Echard, A. (2006). Rab35 regulates an endocytic recycling pathway essential for the terminal steps of cytokinesis. *Curr. Biol.* *16*, 1719–1725.

- Kunda, P., Pelling, A. E., Liu, T., and Baum, B. (2008). Moesin controls cortical rigidity, cell rounding, and spindle morphogenesis during mitosis. *Curr. Biol.* *18*, 91–101.
- Li, W. M., Webb, S. E., Lee, K. W., and Miller, A. L. (2006). Recruitment and SNARE-mediated fusion of vesicles in furrow membrane remodeling during cytokinesis in zebrafish embryos. *Exp. Cell Res.* *312*, 3260–3275.
- Maddox, A. S., Habermann, B., Desai, A., and Oegema, K. (2005). Distinct roles for two *C. elegans* anillins in the gonad and early embryo. *Development* *132*, 2837–2848.
- Maddox, A. S., Lewellyn, L., Desai, A., and Oegema, K. (2007). Anillin and the septins promote asymmetric ingression of the cytokinetic furrow. *Dev. Cell* *12*, 827–835.
- Magie, C. R., Pinto-Santini, D., and Parkhurst, S. M. (2002). Rho1 interacts with p120ctn and alpha-catenin, and regulates cadherin-based adherens junction components in *Drosophila*. *Development* *129*, 3771–3782.
- Marois, E., Mahmoud, A., and Eaton, S. (2006). The endocytic pathway and formation of the Wingless morphogen gradient. *Development* *133*, 307–317.
- Meng, W., Mushika, Y., Ichii, T., and Takeichi, M. (2008). Anchorage of microtubule minus ends to adherens junctions regulates epithelial cell-cell contacts. *Cell* *135*, 948–959.
- Miller, K. G., Field, C. M., and Alberts, B. M. (1989). Actin-binding proteins from *Drosophila* embryos: a complex network of interacting proteins detected by F-actin affinity chromatography. *J. Cell Biol.* *109*, 2963–2975.
- Miyoshi, J., and Takai, Y. (2008). Structural and functional associations of apical junctions with cytoskeleton. *Biochim. Biophys. Acta* *1778*, 670–691.
- Murthy, K., and Wadsworth, P. (2005). Myosin-II-dependent localization and dynamics of F-actin during cytokinesis. *Curr. Biol.* *15*, 724–731.
- Nagafuchi, A., Ishihara, S., and Tsukita, S. (1994). The roles of catenins in the cadherin-mediated cell adhesion: functional analysis of E-cadherin-alpha catenin fusion molecules. *J. Cell Biol.* *127*, 235–245.
- Neufeld, T. P., and Rubin, G. M. (1994). The *Drosophila* *peanut* gene is required for cytokinesis and encodes a protein similar to yeast putative bud neck filament proteins. *Cell* *77*, 371–379.
- Niewiadomska, P., Godt, D., and Tepass, U. (1999). DE-Cadherin is required for intercellular motility during *Drosophila* oogenesis. *J. Cell Biol.* *144*, 533–547.
- O'Farrell, F., and Kylsten, P. (2008). *Drosophila* Anillin is unequally required during asymmetric cell divisions of the PNS. *Biochem. Biophys. Res. Commun.* *369*, 407–413.
- Oda, H., and Tsukita, S. (2001). Real-time imaging of cell-cell adherens junctions reveals that *Drosophila* mesoderm invagination begins with two phases of apical constriction of cells. *J. Cell Sci.* *114*, 493–501.
- Oda, H., Uemura, T., Harada, Y., Iwai, Y., and Takeichi, M. (1994). A *Drosophila* homolog of cadherin associated with armadillo and essential for embryonic cell-cell adhesion. *Dev. Biol.* *165*, 716–726.
- Oegema, K., Savoian, M. S., Mitchison, T. J., and Field, C. M. (2000). Functional analysis of a human homologue of the *Drosophila* actin binding protein anillin suggests a role in cytokinesis. *J. Cell Biol.* *150*, 539–552.
- Pelham, R. J., and Chang, F. (2002). Actin dynamics in the contractile ring during cytokinesis in fission yeast. *Nature* *419*, 82–86.
- Pfeiffer, S., Alexandre, C., Calleja, M., and Vincent, J. P. (2000). The progeny of *wingless*-expressing cells deliver the signal at a distance in *Drosophila* embryos. *Curr. Biol.* *10*, 321–324.
- Piekny, A. J., and Glotzer, M. (2008). Anillin is a scaffold protein that links RhoA, actin, and myosin during cytokinesis. *Curr. Biol.* *18*, 30–36.
- Pirrotta, V. (1988). Vectors for P-mediated transformation in *Drosophila*. *Biotechnology* *10*, 437–456.
- Polevoy, G., Wei, H. C., Wong, R., Szentpetery, Z., Kim, Y. J., Goldbach, P., Steinbach, S. K., Balla, T., and Brill, J. A. (2009). Dual roles for the *Drosophila* PI 4-kinase Four wheel drive in localizing Rab11 during cytokinesis. *J. Cell Biol.* *187*, 847–858.
- Rappaport, R. (1996). *Cytokinesis in Animal Cells*, Cambridge, United Kingdom: Cambridge University Press.
- Riggleman, B., Schedl, P., and Wieschaus, E. (1990). Spatial expression of the *Drosophila* segment polarity gene *armadillo* is posttranscriptionally regulated by *wingless*. *Cell* *63*, 549–560.
- Rodal, A. A., Kozubowski, L., Goode, B. L., Drubin, D. G., and Hartwig, J. H. (2005). Actin and septin ultrastructures at the budding yeast cell cortex. *Mol. Biol. Cell* *16*, 372–384.
- Rodriguez-Escudero, I., Roelants, F. M., Thorner, J., Nombela, C., Molina, M., and Cid, V. J. (2005). Reconstitution of the mammalian PI3K/PTEN/Akt pathway in yeast. *Biochem. J.* *390*, 613–623.
- Romrell, L. J., Stanley, H. P., and Bowman, J. T. (1972). Genetic control of spermiogenesis in *Drosophila melanogaster*: an autosomal mutant (*ms(2)3R*) demonstrating failure of meiotic cytokinesis. *J. Ultrastruct. Res.* *38*, 563–577.
- Royou, A., Sullivan, W., and Kares, R. (2002). Cortical recruitment of non-muscle myosin II in early syncytial *Drosophila* embryos: its role in nuclear axial expansion and its regulation by Cdc2 activity. *J. Cell Biol.* *158*, 127–137.
- Sambrook, J., Fritsch, E. F., and Maniatis, T. (1989). *Molecular Cloning: A Laboratory Manual*, Cold Spring Harbor, NY: Cold Spring Harbor Laboratory Press.
- Sato, N., Yonemura, S., Obinata, T., and Tsukita, S. (1991). Radixin, a barbed end-capping actin-modulating protein, is concentrated at the cleavage furrow during cytokinesis. *J. Cell Biol.* *113*, 321–330.
- Satterwhite, L. L., and Pollard, T. D. (1992). Cytokinesis. *Curr. Opin. Cell Biol.* *4*, 43–52.
- Schmidt, K., and Nichols, B. J. (2004). A barrier to lateral diffusion in the cleavage furrow of dividing mammalian cells. *Curr. Biol.* *14*, 1002–1006.
- Shaner, N. C., Campbell, R. E., Steinbach, P. A., Giepmans, B. N., Palmer, A. E., and Tsien, R. Y. (2004). Improved monomeric red, orange and yellow fluorescent proteins derived from *Discosoma* sp. red fluorescent protein. *Nat. Biotechnol.* *22*, 1567–1572.
- Silverman-Gavrila, R. V., Hales, K. G., and Wilde, A. (2008). Anillin-mediated targeting of peanut to pseudocleavage furrows is regulated by the GTPase Ran. *Mol. Biol. Cell* *19*, 3735–3744.
- Sohrmann, M., Fankhauser, C., Brodbeck, C., and Simanis, V. (1996). The *dmf1/mid1* gene is essential for correct positioning of the division septum in fission yeast. *Genes Dev.* *10*, 2707–2719.
- Somma, M. P., Fasulo, B., Cenci, G., Cundari, E., and Gatti, M. (2002). Molecular dissection of cytokinesis by RNA interference in *Drosophila* cultured cells. *Mol. Biol. Cell* *13*, 2448–2460.
- Straight, A. F., Field, C. M., and Mitchison, T. J. (2005). Anillin binds nonmuscle myosin II and regulates the contractile ring. *Mol. Biol. Cell* *16*, 193–201.
- Takeichi, M. (1995). Morphogenetic roles of classic cadherins. *Curr. Opin. Cell Biol.* *7*, 619–627.
- Takezawa, P. A., DeRisi, J. L., Wilhelm, J. E., and Vale, R. D. (2000). Plasma membrane compartmentalization in yeast by messenger RNA transport and a septin diffusion barrier. *Science* *290*, 341–344.
- Tanaka-Takiguchi, Y., Kinoshita, M., and Takiguchi, K. (2009). Septin-mediated uniform bracing of phospholipid membranes. *Curr. Biol.* *19*, 140–145.
- Tasto, J. J., Morrell, J. L., and Gould, K. L. (2003). An anillin homologue, Mid2p, acts during fission yeast cytokinesis to organize the septin ring and promote cell separation. *J. Cell Biol.* *160*, 1093–1103.
- Weis, W. I., and Nelson, W. J. (2006). Re-solving the cadherin-catenin-actin conundrum. *J. Biol. Chem.* *281*, 35593–35597.
- Wilson, K. L., Fitch, K. R., Bafus, B. T., and Wakimoto, B. T. (2006). Sperm plasma membrane breakdown during *Drosophila* fertilization requires sneaky, an acrosomal membrane protein. *Development* *133*, 4871–4879.
- Wong, R., Fabian, L., Forer, A., and Brill, J. A. (2007). Phospholipase C and myosin light chain kinase inhibition define a common step in actin regulation during cytokinesis. *BMC Cell Biol.* *8*, 15.
- Wong, R., Hadjiyanni, I., Wei, H. C., Polevoy, G., McBride, R., Sem, K. P., and Brill, J. A. (2005). PIP₂ hydrolysis and calcium release are required for cytokinesis in *Drosophila* spermatocytes. *Curr. Biol.* *15*, 1401–1406.
- Zacharias, D. A., Violin, J. D., Newton, A. C., and Tsien, R. Y. (2002). Partitioning of lipid-modified monomeric GFPs into membrane microdomains of live cells. *Science* *296*, 913–916.
- Zhang, J., Kong, C., Xie, H., McPherson, P. S., Grinstein, S., and Trimble, W. S. (1999). Phosphatidylinositol polyphosphate binding to the mammalian septin H5 is modulated by GTP. *Curr. Biol.* *9*, 1458–1467.
- Zhao, W. M., and Fang, G. (2005). Anillin is a substrate of anaphase-promoting complex/cyclosome (APC/C) that controls spatial contractility of myosin during late cytokinesis. *J. Biol. Chem.* *280*, 33516–33524.